A new scheme for calculating soil thermal diffusivity

Yujie Li
Northwest Institute of Eco-Environment and Resources
Xiaoqing Gao (xqgao@lzb.ac.cn)
Northwest Institute of Eco-Environment and Resources https://orcid.org/0000-0003-0806-2014
Liwei Yang
Northwest Institute of Eco-Environment and Resources
Zhenchao Li
Northwest Institute of Eco-Environment and Resources
Ya Zhou
Qufu Normal University

Research Article

Keywords: Land-atmosphere interaction, land surface process, Soil temperature, Soil thermal diffusivity,Thermal conductivity-convection equation

Posted Date: March 29th, 2022

DOI: https://doi.org/10.21203/rs.3.rs-1457633/v1

A new scheme for calculating soil thermal diffusivity

Yujie Li [1,2] · Xiaoqing Gao [1,2*] · Liwei Yang[1,2] · Zhenchao Li[1,2] · Ya Zhou[3]

[1]Key Laboratory of Land Surface Process and Climate Change in Cold and Arid Regions of Chinese Academy of Sciences, Northwest Institute of Eco-Environment and Resources, Chinese Academy of Sciences, Lanzhou, Gansu, 730000, China.

[2]University of Chinese Academy of Sciences, Beijing 100049, China.

[3]Qufu Normal University, Rizhao, Shandong, 276826, China.

Corresponding author： Xiaoqing Gao. Email: xqgao@lzb.ac.cn

Acknowledgments

Financial support from the National Key R&D Program of China (2018YFB1502800), the National Natural Science Foundation of China (Grant No. 41875017) and the Opening Fund of Key Laboratory of Desert and Desertification, CAS (No. KLDD-2020-004) is gratefully acknowledged. The authors declare no competing financial interest. The authors would also like to thank the anonymous reviewers for their constructive comments and suggestions that significantly improved the quality of our manuscript.

Declarations

Conflict of interest The authors declare that they have no competing interest.

Abstract

Land-atmosphere interaction is one of the important causes of climate change. The accurate characterization of physical mechanism of the soil layer can help us better understand the land-atmosphere interaction. As one of the important thermal properties of soil, soil thermal diffusivity is an important parameter reflecting soil thermal conductivity and a necessary condition for simulating soil thermodynamic environment. Based on the comparison of several methods for calculating soil thermal diffusivity (amplitude method, phase method, logarithmic method, arctangent method, Laplace method and numerical methods), this paper develops a new soil thermal diffusivity model (Thermal conduction-convection method based on Fourier series boundary condition for calculating soil thermal diffusivity, TCCMF) and compares the results of the new model with other methods. The results show that: (1) The accuracy of the results obtained by the amplitude method, phase method, logarithmic method, and arctangent method is not high enough; the Laplace method can better solve the effects of extreme weather or non-periodic changes in soil temperature. (2) When the numerical methods are used to solve the thermal conduction equation, the Crank-Nichalson-Sch format is unconditionally stable, the data utilization rate is higher, the obtained soil thermal diffusivity is less discrete, and the result is more accurate. (3) The new model (TCCMF) uses the Fourier series method, which is easy to calculate, and has more complete physical process and more flexible precision control. The simulation results of soil temperature using this method show that this method (TCCMF) has better simulation accuracy, indicating that it has potential value in simulating soil thermodynamic characteristics and land-atmosphere interaction.

Keywords Land-atmosphere interaction · land surface process · Soil temperature · Soil thermal diffusivity ·Thermal conductivity-convection equation

1 Introduction

The interaction of earth sphere layers is a prominent feature of contemporary earth science thought. Climate change is the result of the interaction of earth sphere layers. Surface processes are various physical, chemical, and biological processes that occur at the earth-air interface, and are the embodiment of the interaction between the pedosphere, hydrosphere, atmosphere, and biosphere. Humans live on land, and the land-atmosphere interaction (mass and energy

exchange) profoundly affects the living environment of human beings. A lot of studies have been done on land-atmosphere interaction and its climate effects.For example, the land-atmosphere interaction increases the climate variability in Central and Eastern Europe, and the increase in summer temperature is also due to the feedback effect between the surface and the atmosphere (Seneviratne et al. 2006). The Global Energy and Water Cycle Experiment (GEWEX) Continental –Scale International Project (GCIP) improved the accuracy and sophistication of land-surface schemes in many national models, defined water budgets for the central United States and provided a new understanding of dynamics of regional energy and water budgets (Lawford 1999). The First International Satellite Land Surface Climatology Porject (ISLSCP) studied surface forcing of planetary boundary layer circulations, surface flux modeling-parameterization–retrieval methods, biotic effects on boundary layer processes, remote sensing of surface properties, and so on (Smith 1998; Williams et al. 2019). NOPEX (a Northern Hemisphere Climate Processes Land Surface Experiment) pointed out the importance of the boreal forests and studied surface-atmosphere interactions in forest-dominated landscapes in northern Europe (Halldin et al. 1998). Heihe River Basin Field Experiment (HEIFE) pointed out that the land-atmosphere interaction is realized through the exchange of energy and mass on the earth's surface, the exchange of mass and energy between the land surface and atmosphere is realized through the planetary boundary layer process (Hu and Gao 1994; Hu et al. 1994). Soil layers are important in land-atmosphere interactions. The mass and energy exchange between land and atmosphere is realized through the soil layer. The understanding of the physical and chemical properties of the soil layer directly determines our grasp of the land-atmosphere interaction. Due to the large spatial heterogeneity of soils, we still have insufficient understanding of the spatial heterogeneity of soils and their temporal changes. Thermal properties are one of the important properties of soils, which control the transfer and storage of heat in soils. Soil thermal diffusivity is an important parameter to characterize soil thermal properties, it represents the propagation speed of temperature waves in soil (Zhang et al. 2011). Together with the soil temperature gradient, it also controls the magnitude of soil heat flow. Therefore, the accurate inversion of soil thermal diffusivity is of great significance for understanding soil thermodynamic-dynamic processes and land-atmosphere interactions.

The soil thermal diffusivity is usually defined as $k = \lambda / C_g$, which is determined by the volumetric heat capacity of the soil C_g (unit: $J \cdot cm^{-3} \cdot K^{-1}$) and the soil thermal conductivity λ

(unit: $\mathrm{W} \cdot m^{-1} \cdot K^{-1}$). It is difficult to directly observe the soil thermal diffusivity, so it is generally obtained by inversion. The thermal diffusivity can be determined based on the observed soil temperature in a variety of ways, most of which are based on the assumption that soil is a semiunbounded medium with a constant thermal diffusivity and that the upper thermal boundary can be expressed by a harmonic function (Li et al. 2015; Zheng and Liu 2013). In terms of the thermal conduction equation for soil temperature (SCM), the common calculation methods include the amplitude method, phase method, arctangent method, logarithmic method, numerical method, harmonic method, Laplace method, and modified Laplace method (Bhumralkar 1975). The amplitude method, phase method, arctangent method, logarithm method, and harmonic method assume that the soil temperature at the boundary is in the form of a sine function or Fourier series. Evaluation of these methods shows that the Fourier series is the most reliable one. For the non-periodic soil temperature, the boundary conditions of the soil temperature obtained by the Laplace method and the improved Laplace method are closer to the real soil thermal conduction process, but the two methods are very complicated in calculation (Liu et al. 2014).

There are three ways of heat transfer, namely conduction, convection and radiation. Under actual soil conditions, the vertical water vapor flux will also affect the soil temperature through convection, so the thermal conduction-convection equation (SCCM) will make the calculation results more accurate. Studies have shown that, compared with the thermal conduction equation (SCM), the difference between the soil thermal diffusivity calculated using the thermal conduction-convection equation (SCCM) and the measured one is smaller (Goto et al. 2005; Kane et al. 2001). Fan and Tang (1994) derived the expression of the thermal conduction-convection equation, solved the soil thermal diffusivity and heat flux according to its physical mechanism, and analyzed the relationship between heat flux and earthquake. Gao et al. (2005) solved the analytical solution of the thermal conduction-convection equation by mathematical methods, and obtained the same expression as Fan and Tang (1994). However, the previous scholars assumed that the soil temperature at the boundary is a sine function when doing the derivation, which may not be accurate enough in the process of describing the soil temperature and solving the soil thermal diffusivity.

Since the 20th century, scholars have proposed many methods for calculating the thermal diffusivity of soil. Whether based on SCMs, SCCMs, or different soil thermodynamic properties,

these methods have their own applicable conditions, advantages and disadvantages. Previous work led to important contributions, although the horizontal comparison of various methods was relatively insufficient. Therefore, the objectives of the present study were to (1) transversely compare the results of soil thermal diffusivity obtained from different boundary conditions under the SCM; (2) derive a method of solving the SCCM under the condition of a Fourier boundary and obtain the thermal diffusivity; (3) compare the measured soil temperature with the soil temperature obtained by solving the SCCM under the Fourier boundary condition. The research not only provides a more accurate simulation of soil temperature and a useful tool for calculating soil thermal diffusivity, but also partially analyzes the thermal fluctuations in the soil. It helps to understand the changes in soil thermal properties and thermal movement, as well as the land-atmosphere interaction under the background of climate change.

2 Field experiments

The observation site is located in Golmud. Golmud is composed of two unconnected parts: the central and southern parts of the Qaidam Basin and Tanggula Mountain. The average temperature in Golmud is 5.3 °C, the precipitation is 42.1 mm, the relative humidity is 32%, the cumulative number of sunshine events is 3096.3 h, and the accumulated annual evaporation is 2504.1 mm. It belongs to the continental plateau climate and presents less rain, wind and drought. The annual average sunshine hours in the region are 3200~3600 h, and the annual total solar radiation is 6618~7356 MJ/m^2. It is the second largest high-value solar radiation area in China after the Qinghai-Tibet Plateau (Yang et al. 2017).The soil temperature used in this study was recorded every 10 minutes by CR1000 produced by Campbell Corporation of the United States at 6 depth layers of 5 cm, 10 cm, 20 cm, 40 cm, 80 cm, and 180 cm for the period from October 2012 to July 2013. The data were quality controlled (Gao et al. 2016).

3 Method

3.1 Thermal conduction equation for soil temperature (SCM)

The volumetric heat capacity C_g($\mathrm{J}\cdot cm^{-3}\cdot K^{-1}$) and the soil thermal conductivity λ ($\mathrm{W}\cdot m^{-1}\cdot K^{-1}$) are assumed to remain consistent with depth based on the classical thermal diffusion equation in a one-dimensional semiunbounded medium:

$$\frac{\partial \mathrm{T}}{\partial \mathrm{T}} = \mathrm{k}\frac{\partial^2 \mathrm{T}}{\partial \mathrm{z}^2} \qquad (1)$$

where $\mathrm{k} = \lambda/C_g$ (unit: $m^2 s$) is the thermal diffusivity.

The boundary condition at z_1 is given by the following equation (Van Wijk and de Vries, 1963):

$$\mathrm{T}|_{z=z1} = \overline{\mathrm{T_1}} + \mathrm{A_1}\sin(\omega \mathrm{t} - \Phi_1), \mathrm{t} \geq 0 \qquad (2)$$

where $\overline{\mathrm{T_1}}$ (°C) is the average value of soil temperature at depth z_1, $\mathrm{A_1}$ (°C) is the amplitude, ω=2π/p (rad/s) is the daily change period, p is the period of the change, and Φ_1 is the initial soil temperature (primary phase) (rad) at depth z_1, which is obtained by least squares fitting.

According to Eq. (1) and Eq. (2), the soil temperature at depth z_2 is expressed as follows:

$$\mathrm{T}_{z=z2} = \overline{\mathrm{T_2}} + A_1 \exp[(z_1 - z_2)\alpha]\sin[\omega \mathrm{t} - \Phi_1 - (z_2 - z_1)\alpha] \qquad (3)$$

where $\alpha = \sqrt{\omega/2\mathrm{k}}$. The amplitude $\mathrm{A_2}$ and initial phase Φ_2 at depth z_2 are as follows:

$$\mathrm{A_2} = \mathrm{A_1}\exp[-(z_2 - z_1)\alpha]$$

$$\Phi_2 = \Phi_1 + (\mathrm{z_2} - \mathrm{z_1})\alpha$$

According to Eq. (1) to Eq. (3), the thermal diffusivity k can be expressed with the amplitude and phase:

$$\mathrm{k}_P = (\mathrm{z_1} - \mathrm{z_2})^2\,\omega/[2(\Phi_1 - \Phi_2)^2] \qquad (4)$$

$$\mathrm{k}_A = (\mathrm{z_1} - \mathrm{z_2})^2\,\omega/[2\ln^2(\mathrm{A_1}/\mathrm{A_2})] \qquad (5)$$

3.1.1 Arctangent method and logarithmic method

Soil temperatures can be simulated with a series of sinusoidal terms. Observations of soil temperature at a certain depth can be expressed in Fourier series:

$$\mathrm{T}(\mathrm{t}) = \overline{\mathrm{T}} \cdot \sum_{n=1}^{2}[\mathrm{A_n}\cos(\mathrm{n}\omega \mathrm{t}) + \mathrm{B_n}\sin(\mathrm{n}\omega \mathrm{t})] \qquad (6)$$

where $\overline{T}$ (°C) is the average value of soil temperature and A_n and B_n (°C) are amplitudes. Eight soil temperature observations were performed at two depths per day. The phase method is shown in Eq. (4):

$$k = \omega(z_1 - z_2)^2 \cdot \{2\{\arctan \left[\frac{(T_1(z_1) - T_3(z_1))(T_2(z_2) - T_4(z_2)) - (T_2(z_1) - T_4(z_1))(T_1(z_2) - T_3(z_2))}{(T_1(z_1) - T_3(z_1))(T_1(z_2) - T_3(z_2)) + (T_2(z_2) - T_4(z_1))(T_2(z_2) - T_4(z_2))}\right]\}^2\}^{-1} \quad (7)$$

where $T_1(z_1)$, $T_2(z_1)$, $T_3(z_1)$, $T_4(z_1)$ and $T_1(z_2)$, $T_2(z_2)$, $T_3(z_2)$, $T_4(z_2)$ are four soil temperature observations at z_1 and z_2.

The amplitude method is shown in Eq. (5):

$$k = \frac{\omega}{2} \times \frac{z_2 - z_1}{\{\ln\left[\frac{(T_1(z_1) - T_3(z_1))^2 + (T_2(z_1) - T_4(z_1))^2}{((T_1(z_2) - T_3(z_2)))^2 + (T_2(z_2) - T_4(z_2))^2}\right]\}^2} \quad (8)$$

Eq. (7) is an arctangent method, and Eq. (8) is a logarithmic method, which was developed early without automatic recording equipment. Compared with the phase method in Eq. (4) and amplitude method in Eq. (5), the arctangent method and the logarithmic method do not need to fit the amplitude and phase; thus, they are simpler and more convenient to use and have the ability to reflect the possible nonsinusoidal changes (Liu et al.,1991). However, the temperature sampling data at intervals of 6 h will inevitably lead to the absence of short-period signals. When the heat transfer model is established, there are no high-order harmonic components with boundary conditions, which leads to further errors in the simulation results (Liu et al. 2014).

3.1.2 Laplace transformation based method (LTM)

In Section (3.1.1), the prerequisite for the four methods is to assume a stable cyclical change in soil temperature. In actual circumstances, if there is a sudden change in weather conditions, such as heavy precipitation, cold waves, blizzards, etc., then the stability cycle will fail. Therefore, the model with stable period change as the boundary condition will not be applicable when simulating soil temperature change and obtaining thermal diffusivity (Liu et al. 2014). To better simulate the nonperiodic changes in soil temperature and make the boundary conditions of the model closer to the soil heat transfer process, the Laplace transform is a good choice.

The solution of Eq. (1) with initial and boundary conditions is given as follows:

$$T(z, 0) = T_0 \quad (9a)$$

$$T(0, t) = \Phi(t), t > 0 \quad (9b)$$

Then, the Laplace transformation can be performed (Carslaw and Jaeger, 1959):

$$T(z,t) = T_0 + \frac{z}{2\sqrt{\pi k}}\int_0^t \Phi(\tau)\frac{\exp(\frac{-z^2}{4k(t-\tau)})}{(t-\tau)^{3/2}}d\tau \qquad (10)$$

Eq. (10) applies to a semi-infinite medium whose upper boundary condition is given by Φ(t), a continuous function of time. It is an impulse response equation that is useful for sudden changes in temperature input signals (such as in rainy or cold front transit). A limitation of using this equation is that the initial temperature profile must be uniform. The soil thermal diffusivity can be obtained by fitting Eq. (10) (de Silans et al. 1996).

3.1.3 Numerical method

For homogeneous soils, the heat transfer equation can be approximated by a difference equation. Commonly used differential formats are as follows (Liu et al. 1991):

(1) Dufeat-Frankel-Sch (format 1)

$$\frac{T_j^{n+1} - T_j^n}{2} = \frac{k\Delta t}{\Delta z^2}\left(T_{j+1}^n + T_{j-1}^n - T_j^{n+1} - T_j^{n-1}\right) \qquad (11)$$

This format is stable.

(2) Crank-Nichalson-Sch (format 2)

$$T_j^{n+1} - T_j^n = \frac{k\Delta t}{2\Delta z^2}\left[\left(T_{j+1}^{n+1} - 2T_j^{n+1} + T_{j-1}^{n+1}\right) + \left(T_{j+1}^n - 2T_j^n + T_{j-1}^n\right)\right] \qquad (12)$$

This format is unconditionally stable. In Eq. (11)-(12), j represents a spatial interval and n represents a time interval.

3.2 Thermal conduction-convection equation for soil temperature (SCCM)

Eq. (1) assumes that the soil is vertically uniform. However, some scholars (Gao et al. 2003) believe that the difference between day and night temperature and solar radiation will trigger the vertical movement of soil water, which affects the temperature distribution in soil. To reflect the influence of this part, thermal conduction was combined with convection to establish a soil thermal conduction-convection model:

$$\frac{\partial T}{\partial t} = k\frac{\partial^2 T}{\partial z^2} - \frac{C_W}{C_g}w\theta\frac{\partial T}{\partial z} \qquad (13)$$

where w (m/s) is the liquid flow rate (downward positive), θ is the volumetric water content of the soil, and C_W ($J°C^{-1}m^{-3}$) is the specific heat capacity of the water. Assume that these quantities are independent of z and $-\frac{C_W}{C_g}w\theta$ is the liquid water flux density. Let $W = -\frac{C_W}{C_g}w\theta\frac{\partial T}{\partial z}$, then:

$$\frac{\partial T}{\partial t} = k\frac{\partial^2 T}{\partial z^2} + W\frac{\partial T}{\partial z} \qquad (14)$$

3.2.1 Boundary condition as a superposition of a sine wave on the constant temperature field

Given the following boundary condition:

$$T|_{z=0} = \overline{T} + A\sin\omega t\ (t \geq 0)$$

The solution of Eq. (14) is as follows:

$$T(z,t) = T_0 + A\exp\left[\left(\frac{-W-\alpha}{2k}\right)z\right]\sin\left(\omega t - \Phi_1 - \frac{\beta}{2k}z\right) \qquad (15)$$

where

$$\alpha = \sqrt{\frac{W^2 + \sqrt{W^4 + 16k^2\omega^2}}{2}},\quad \beta = \frac{2\sqrt{2}k\omega}{\sqrt{W^2 + \sqrt{W^4 + 16k^2\omega^2}}} \qquad (16)$$

Therefore, the soil temperature (T) at depth z_2 can be calculated using the following equation:

$$T_{z=z2} = \overline{T_2} + A_1\exp[(z_1 - z_2)\alpha M]\sin[\omega t - \Phi_1 - (z_2 - z_1)\alpha N] \qquad (17)$$

In Eq. (17), M and N can be expressed as follows:

$$M = \frac{\alpha}{\omega}\{W + \frac{1}{\sqrt{2}}[W^2 + (W^4 + \frac{4\omega^4}{\alpha^4})^{1/2}]^{1/2}\}$$

$$N = \sqrt{2}\frac{\omega}{\alpha}[W^2 + (W^4 + \frac{4\omega^4}{\alpha^4})^{1/2}]^{-1/2}$$

Assuming that $z_1 < z_2, A_1 > A_2, \Phi_1 < \Phi_2$, the following equations are derived (Gao, 2005):

$$k = -\frac{(z_2 - z_1)^2\omega\ln(A_2/A_1)}{(\Phi_2 - \Phi_1)[(\Phi_2 - \Phi_1)^2 + \ln^2(A_2/A_1)]} \qquad (18)$$

$$W = \frac{\omega(z_2 - z_1)}{\Phi_2 - \Phi_1}\left[\frac{-(\Phi_2 - \Phi_1)^2 + \ln^2(A_2/A_1)}{(\Phi_2 - \Phi_1)^2 + \ln^2(A_2/A_1)}\right] = \frac{\omega(z_2 - z_1)}{\Phi_2 - \Phi_1}\left[\frac{2\ln^2(A_2/A_1)}{(\Phi_2 - \Phi_1)^2 + \ln^2(A_2/A_1)} - 1\right] \qquad (19)$$

The above is the thermal conduction-convection method.

3.2.2 Boundary condition as the form of Fourier series

Hu et al. (2015) derived the thermal conduction-convection equation for the Fourier series boundary of soil temperature (FCCM). Given the following boundary condition:

$$T(0,t) = T_0 + \sum_{n=1}^{N} A_n \sin(n\omega t - \Phi_n), n = 1,2,\dots,N \qquad (20)$$

where n is the number of harmonics.

The solution of Eq. (15) is as follows:

$$T(z,t) = T_0 + \sum_{n=1}^{N} A_n \times \exp\left[\left(-\frac{W}{2k} - \frac{\sqrt{2}}{4k}X_n\right)z\right] \sin\left(n\omega t - \frac{\sqrt{2}\omega}{nX_n}z\right) \qquad (21)$$

where

$$\alpha_n = \sqrt{\frac{{W_n}^2 + \sqrt{{W_n}^4 + 16{k_n}^2\omega^2}}{2}}, \quad \beta_n = \frac{2\sqrt{2}k_n\omega}{\sqrt{{W_n}^2 + \sqrt{{W_n}^4 + 16{k_n}^2\omega^2}}}$$

Therefore, the soil temperature (T) at depth z_2 can be calculated using the following equation:

$$T_{z=z2} = \overline{T_2} + \sum_{n=1}^{N} A_n \exp\left[\left(\frac{-W - \alpha_n}{2k}\right)(z_2 - z_1)\right] \times \sin\left[n\omega t - \Phi_n - (z_2 - z_1)\frac{\beta_n}{2k}\right] \qquad (22)$$

3.2.3 Soil thermal diffusivity under Fourier boundary conditions($\boldsymbol{k_n}$, TCCMF)

The detailed derivation of k_n is in the appendix.

$$W_n = \frac{\omega(z_1 - z_2)}{n\left(\Phi_n^1 - \Phi_n^2\right)}\left[\frac{2\ln^2\left(\frac{A_n^1}{A_n^2}\right)}{n^2\left(\Phi_n^1 - \Phi_n^2\right)^2 + \ln^2\left(\frac{A_n^1}{A_n^2}\right)} - 1\right] \qquad (23)$$

$$k_n = -\frac{(z_1 - z_2)^2\omega \ln\left(\frac{A_n^1}{A_n^2}\right)}{n\left(\Phi_n^1 - \Phi_n^2\right)\left[n^2\left(\Phi_n^1 - \Phi_n^2\right)^2 + \ln^2\left(\frac{A_n^1}{A_n^2}\right)\right]} \qquad (24)$$

4 Result

4.1 Comparison of five methods for the thermal conduction equation in the shallow soil layer

The soil thermal diffusivities at six depths (5-10 cm, 5-20 cm, 5-40 cm, 10-20 cm, 10-40 cm, and 20-40 cm) in the shallow soil of the photovoltaic power station were calculated by the

amplitude method, phase method, arctangent method, logarithm method and Laplace method. The boundary condition of the amplitude method and the phase method is that a constant sine wave is superimposed on the constant temperature field. Selecting the parts of the fitting result whose judgment coefficients are greater than 0.8 (Wang et al. 2019), Fig. 1c, e and f show that there are fewer data with coefficients of determination greater than 0.8 at 40 cm and the fitting result is not good. Fig. 1 shows that the results obtained by the amplitude method at the four levels of 5-10 cm, 5-20 cm, 5-40 cm, and 10-20 cm are generally larger than that of the phase method. Compared with the amplitude method, the phase method can partially reflect the extreme values of the thermal diffusivity. Fig. 2 shows that the arctangent method is derived from the phase method. In addition, 0, 8, 16 and 24 (Beijing time) points are selected every day and the obtained soil thermal diffusivity results are more uniform. Compared with the phase method, it does not reflect some extreme conditions. The logarithm method is derived from the formula of the amplitude method. The time of selection was based on 0, 8, 16 and 24 (Beijing time) points. The results obtained by the logarithm method are similar to those obtained by the amplitude method. However, some extreme values reflected by the amplitude method are not reflected in the logarithmic method. At depths of 5-40 cm, the soil thermal diffusivity obtained by the amplitude method, the phase method, the arctangent method and the logarithm method have large differences. The Laplace method does not have a formula for the established boundary conditions. Fig. 3 shows that the method is effective in reflecting the influence of some extreme conditions and nonperiodic weather changes on the thermal diffusivity. The above results are basically consistent with the results obtained by Liu et al. (1991). The amplitude method and phase method are based on a single temperature sine wave, which is used to describe the general soil, and the accuracy is not high enough, especially when there are multiple extreme temperature values. The arctangent method and logarithmic method require less measured data and present more convenient data acquisition, which is one of the main reasons for their lack of precision, and they also inherit some of the disadvantages of the amplitude method and phase method. The Laplace method has no fixed boundary condition function, and it has outstanding advantages in dealing with actual weather conditions, such as sudden weather, heavy precipitation, cold waves, blizzards and other nonperiodic weather changes.

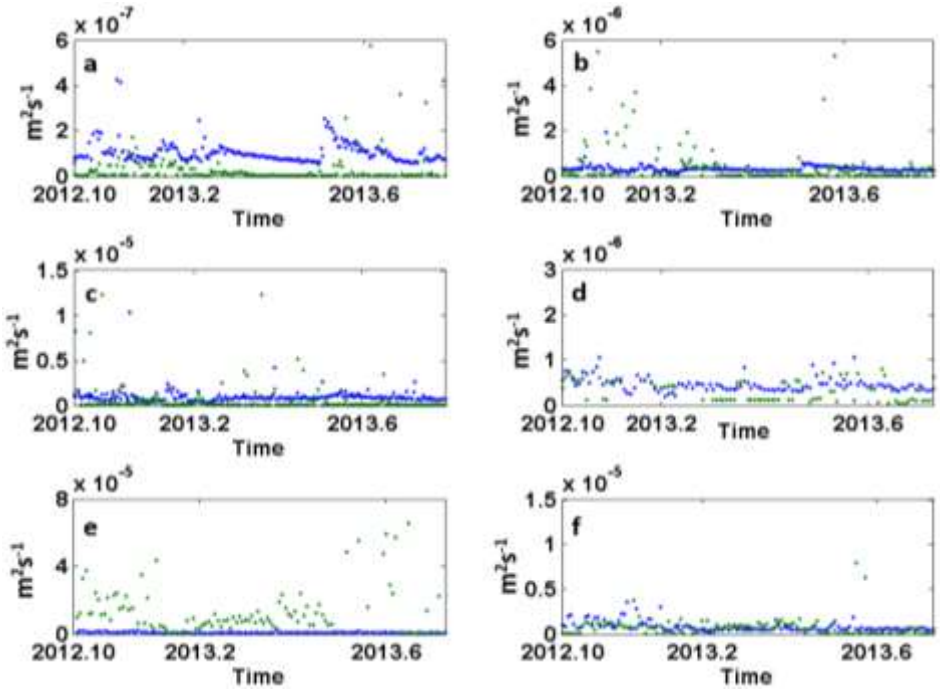

285

286 **Fig. 1** Soil thermal diffusivities at six different depths calculated by the amplitude method and
287 phase method. **a**. 5-10 cm, **b**. 5-20 cm, **c**. 5-40 cm, **d**. 10-20 cm, **e**. 10-40 cm, and **f**. 20-40 cm.
288 Blue represents the amplitude method, and green represents the phase method.

289

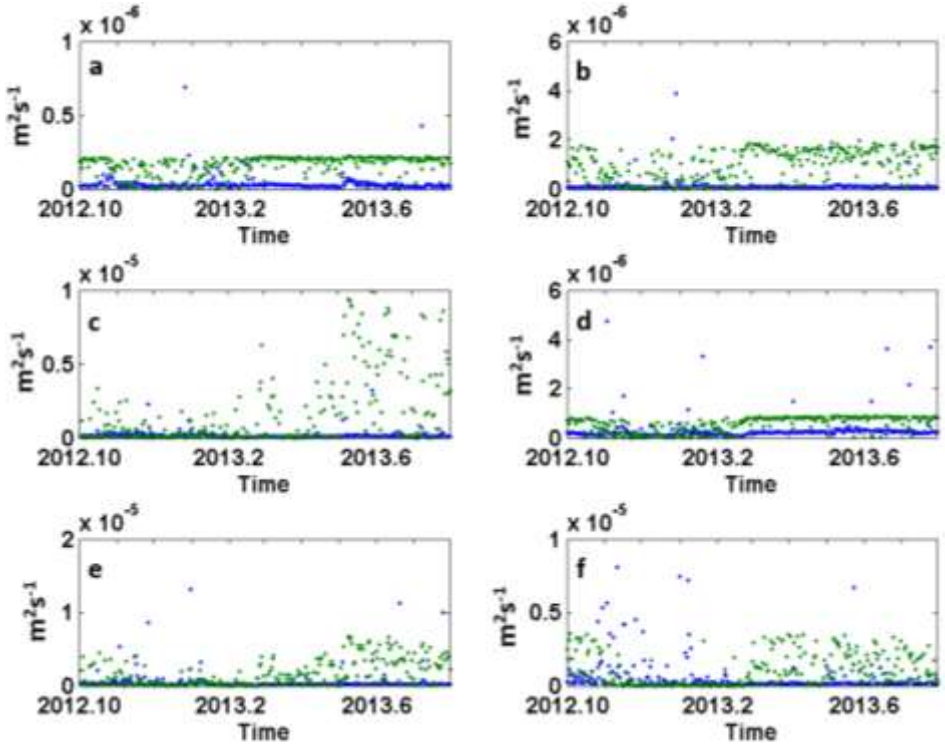

290

291 **Fig. 2** Soil thermal diffusivities at six different depths calculated by the logarithmic method and
292 arctangent method. **a**. 5-10 cm, **b**. 5-20 cm, **c**. 5-40 cm, **d**. 10-20 cm, **e**. 10-40 cm, and **f**. 20-40
293 cm. Blue stands for arctangent, and green stands for logarithm

294

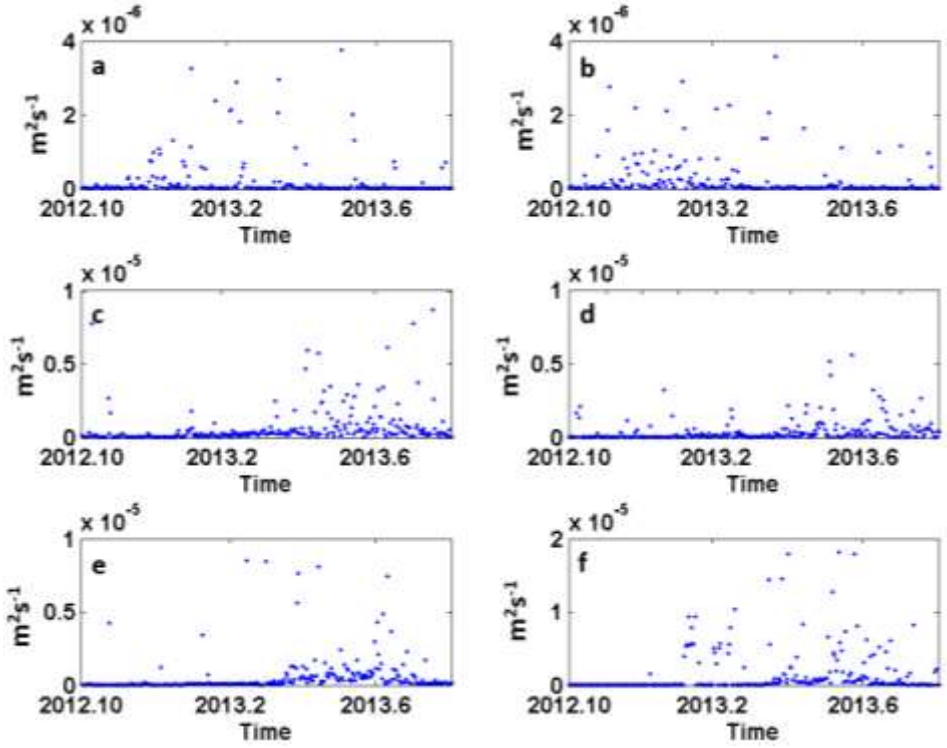

Fig. 3 Soil thermal diffusivities at six different depths calculated by the Laplace method. **a**. 5-10 cm, **b**. 5-20 cm, **c**. 5-40 cm, **d**. 10-20 cm, **e**. 10-40 cm, and **f**. 20-40 cm.

4.2 Analysis of numerical methods for the thermal conduction equation

Two differential formats are used, namely, format 1 (Dufeat-Frankel-Sch) and format 2 (Crank- Nichalson-Sch), and the heat transfer equation is solved in 10-minute steps. The results are shown in Fig. 4. The three different depths (5-20 cm, 5-40 cm, 10-40 cm) of soil thermal diffusivity obtained by the two methods in Fig. 4 have two peaks between December 2012 and June 2013. The thermal diffusivity changes obtained in the two formats are generally the same, but the dispersion of k values in the second format is small. Between the two, although format 1 is stable, the data utilization is less than that of format 2 and the precision is lower. The second format is unconditionally stable, and the data utilization rate is high; therefore, the degree of dispersion is small, and the precision is higher. Liu et al. (1991) pointed out that on a sunny day with few clouds, the numerical method needs to measure 12 data points from 3 depths; and when the weather is cloudy, it is necessary to measure 24 data points from 3 depths with high precision. In the case of a shortened time interval, the relative bias will also decrease; in both

formats, format 2 has higher precision and neither of them needs to reduce Δz or Δt to ensure stability.

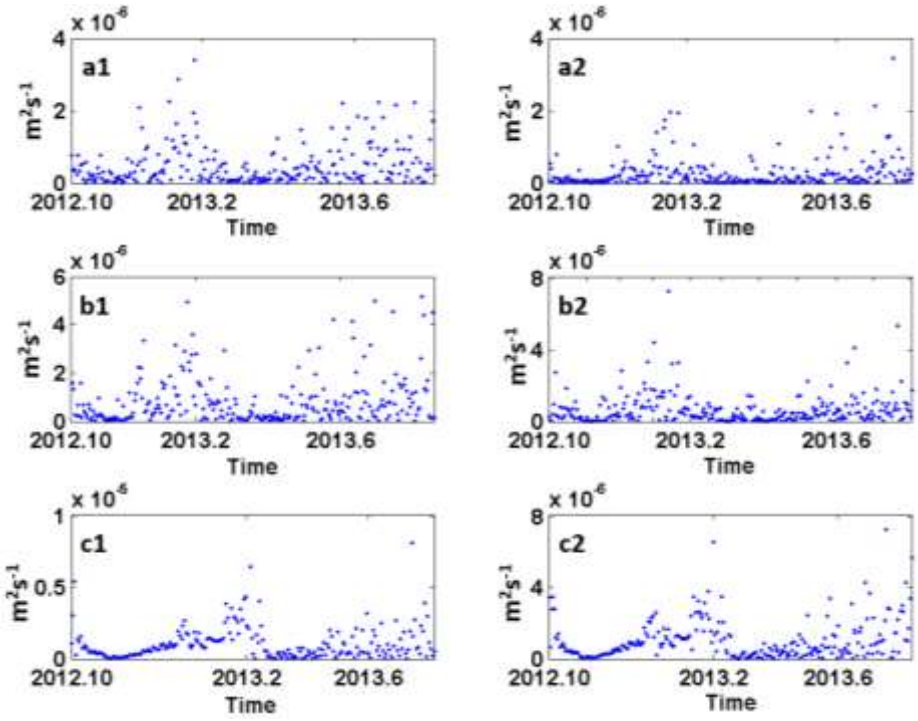

Fig. 4 Soil thermal diffusivities at three different depths calculated by format 1 (Dufeat-Frankel-Sch) and format 2 (Crank-Nichalson-Sch). **a**1, **a**2. 5-20 cm; **b**1, **b**2. 5-40 cm; and **c**1, **c**2. 10-40 cm.

4.3 Analysis of the results of the thermal conduction-convection equation under Fourier series boundary conditions

4.3.1 First-order Fourier series (thermal conduction-convection)

In Fig. 5, the thermal conduction-convection method is a special case (first-order) of the thermal conduction-convection equation under the Fourier boundary condition. Traditional algorithms assume that the soil is vertically uniform and only consider heat transfer; the thermal conduction-convection equation considers the vertical heterogeneity in the soil and combines the effects of upward thermal convection (water transport) on soil temperature. Comparing the results of the thermal conduction-convection method with the previous methods, the thermal conduction-convection method is more sensitive to the change in soil thermal diffusivity and can better reflect the change in soil thermal diffusivity with weather. The main disadvantage of the

traditional thermal conduction equation is that when the vertical gradient of soil thermal diffusivity is relatively large, it overestimates the amplitude and phase of the soil temperature; therefore, it is only suitable for estimating the actual soil temperature of vertically uniform dry soil (Gao 2005).

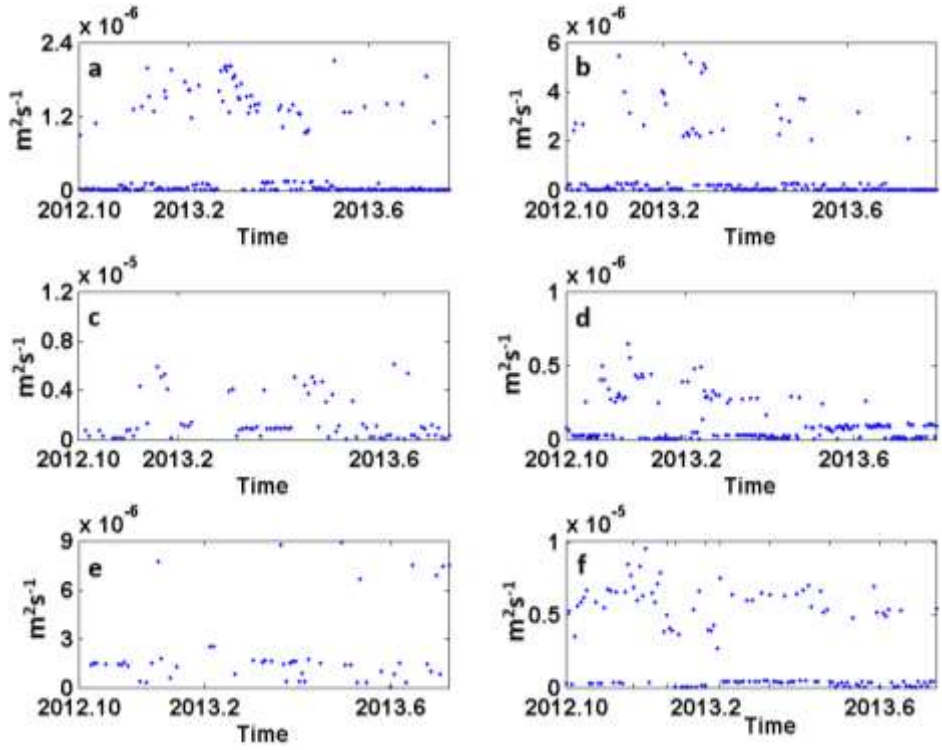

Fig. 5 Soil thermal diffusivities of six different depths on the surface calculated by the first-order Fourier series (thermal conduction-convection method). **a**. 5-10 cm, **b**. 5-20 cm, **c**. 5-40 cm, **d**. 10-20 cm, **e**. 10-40 cm, and **f**. 20-40 cm.

4.3.2 Second-order, third-order and fourth-order Fourier series

In Fig. 6, Fig. 7 and Fig. 8, the Fourier series, which is a special case of the Fourier integral, is one of the classical methods for analyzing the continuity of periodic signals. When performing Fourier series decomposition on a computer, the continuous signal is sampled and then decomposed according to the discrete Fourier series. Any periodic continuous signal can be decomposed into a set of rotation vectors according to the Fourier series (Ahmed and Rao 1975; Liang 1982). The soil thermal diffusivity is difficult to change, and it has a certain periodicity most of the time; therefore, it is reasonable to use the Fourier series. Fourier decomposition is essentially a filtering process (Duan et al. 2016). The fitted nth-order phase Φ_n and the

amplitude A_n are substituted into Eq. (32) to obtain the value of k_n, which is the contribution of different wave components to the soil thermal diffusivity k. These soil thermal diffusivity components k_n can be superimposed to obtain a more accurate change in the soil thermal diffusivity k. As the order n becomes larger, the simulated soil thermal diffusivity k will be more accurate.

Second-order:

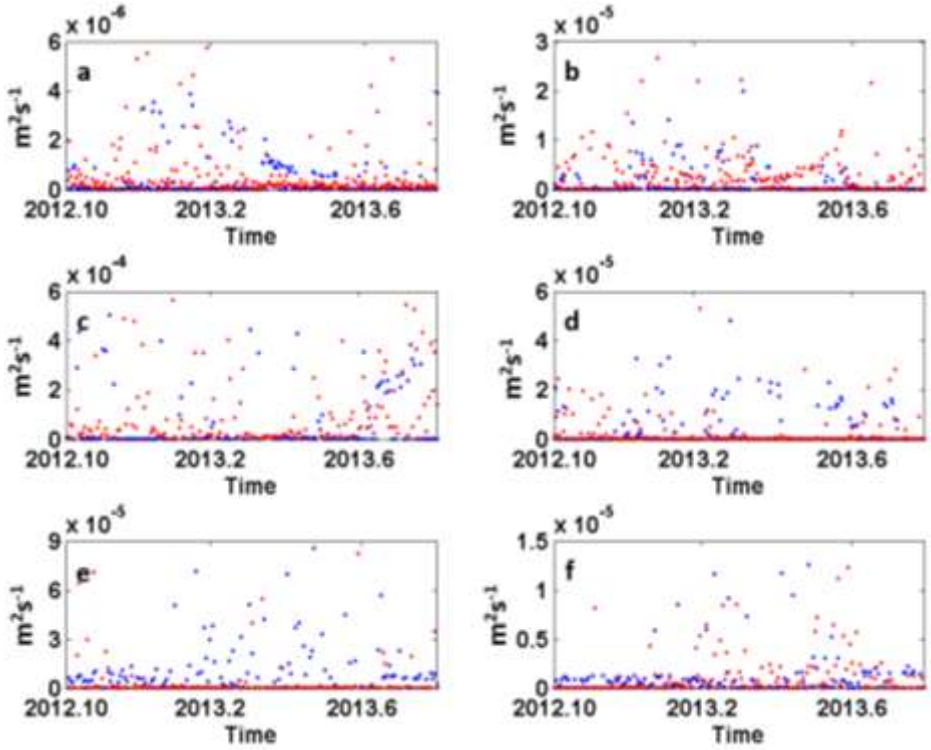

Fig. 6 Soil thermal diffusivities of six different depths on the surface calculated by second-order Fourier series. **a**. 5-10 cm, **b**. 5-20 cm, **c**. 5-40 cm, **d**. 10-20 cm, **e**. 10-40 cm, and **f**. 20-40 cm. Blue for k1, and red for k2.

Third-order:

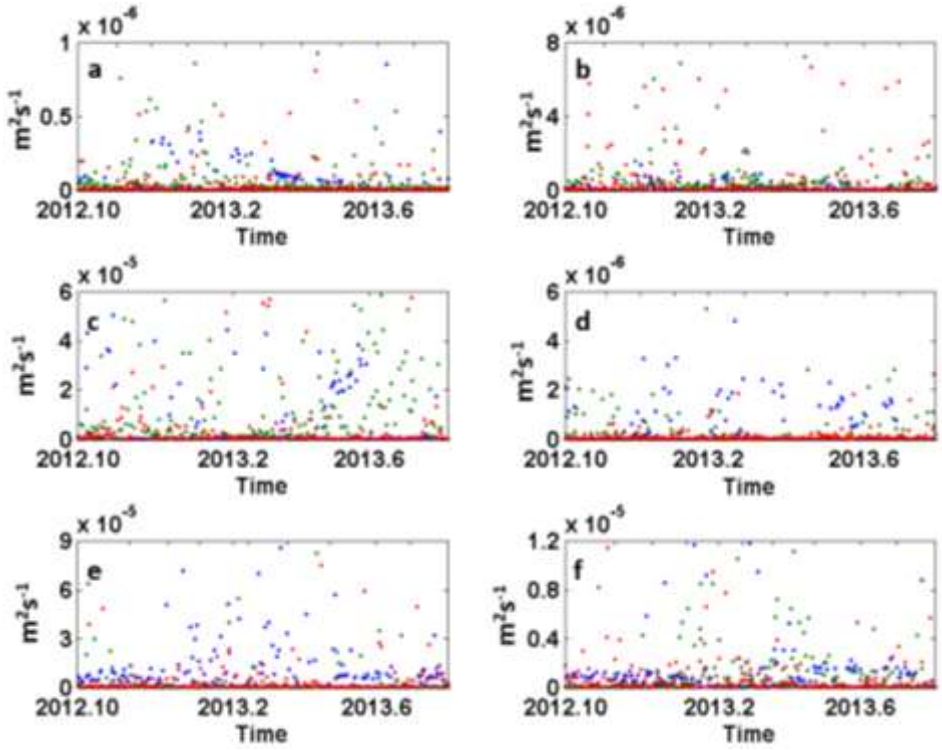

Fig. 7 Soil thermal diffusivities of six different depths on the surface calculated by third-order Fourier series. **a**. 5-10 cm, **b**. 5-20 cm, **c**. 5-40 cm, **d**. 10-20 cm, **e**. 10-40 cm, and **f**. 20-40 cm. Blue for k1, red for k2, and green for k3.

Fourth-order:

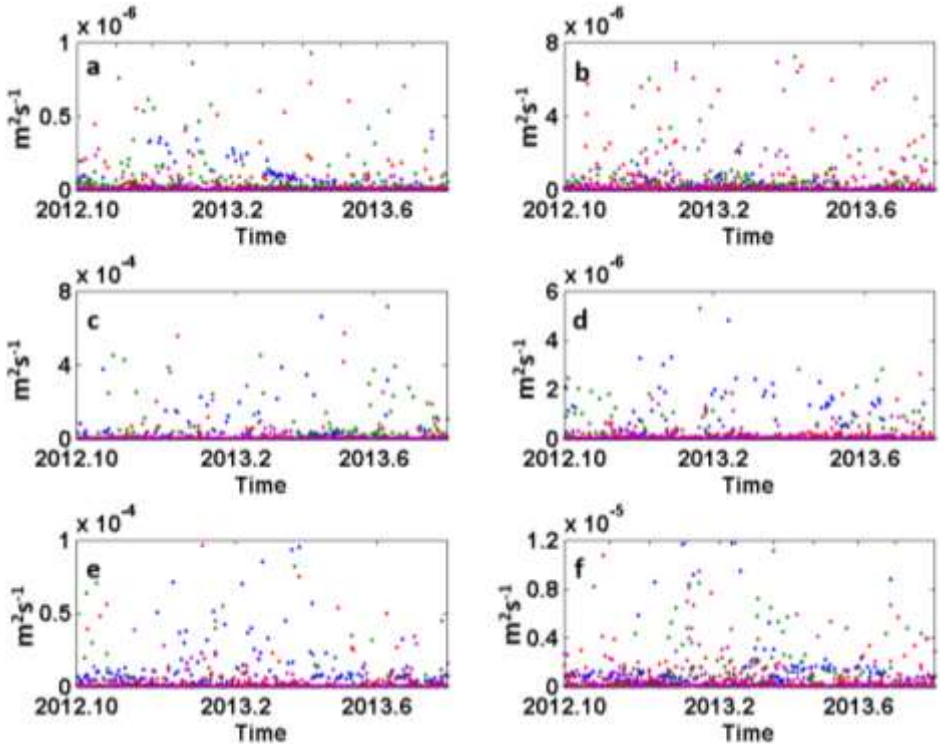

Fig. 8 Soil thermal diffusivities of six different depths on the surface calculated by fourth-order Fourier series. **a**. 5-10 cm, **b**. 5-20 cm, **c**. 5-40 cm, **d**. 10-20 cm, **e**. 10-40 cm, and **f**. 20-40 cm. Blue for k1, red for k2, green for k3, and purple for k4

4.4 Bias analysis of fitting soil temperature under Fourier series

Soil temperature changes are complex and affected by many factors. Soil convective heat exchanges have a significant contribution to soil temperature oscillations. Therefore, using the Fourier series to accurately describe the diurnal variation in shallow soil can reduce the bias caused by assuming that the temperature of the soil surface follows a single sine wave (Wang et al. 2010). In this section, the soil temperature fitted by the 1st-, 2nd-, 3rd-, and 4th-order Fourier series is compared with the measured soil temperature. The goodness of fit of different regression models is usually determined using the coefficient of determination (R^2) (Wang et al. 2019). The coefficient of determination, also known as the determination coefficient, and the decision index represent the amount by which the independent variable explains the percentage change of the dependent variable. Therefore, the larger the coefficient of determination, the better the regression effect of the model. R^2 can be expressed as follows:

$$R^2 = 1 - \frac{\sum(y - \hat{y})^2}{\sum(y - \bar{y})^2}$$

In Fig. 9, several sets of data at the same depth (a1, b1, c1, d1; a2, b2, c2, d2; a3, b3, c3, d3; a4, b4, c4, d4; a5, b5, c5, d5; a6, b6, c6, d6) are used for comparison. In the six sets of data, the R^2 value is ordered as follows fourth-order > third-order > second-order > first-order. In addition, the fourth-order Fourier series is used to fit the soil temperature to depths of 5 cm, 10 cm, and 20 cm, R^2 is above 0.96, and the highest is 0.9999. The minimum value of the fitting result with respect to the first-order Fourier series is less than 0.5, indicating that the fitting result also improves as the fitting order increases. At depths of 80 cm and 180 cm, the soil change was close to a linear change due to the layered soil (Fig. 10); therefore, the results obtained by the Fourier series were weaker than that at other levels. Moreover, studies have shown that using the fifth-order Fourier series to simulate the daily variation in the soil temperature field is quite accurate (Liu et al. 1991). Too many harmonics will cause oscillations, which are not only difficult to calculate but also reduce the accuracy.

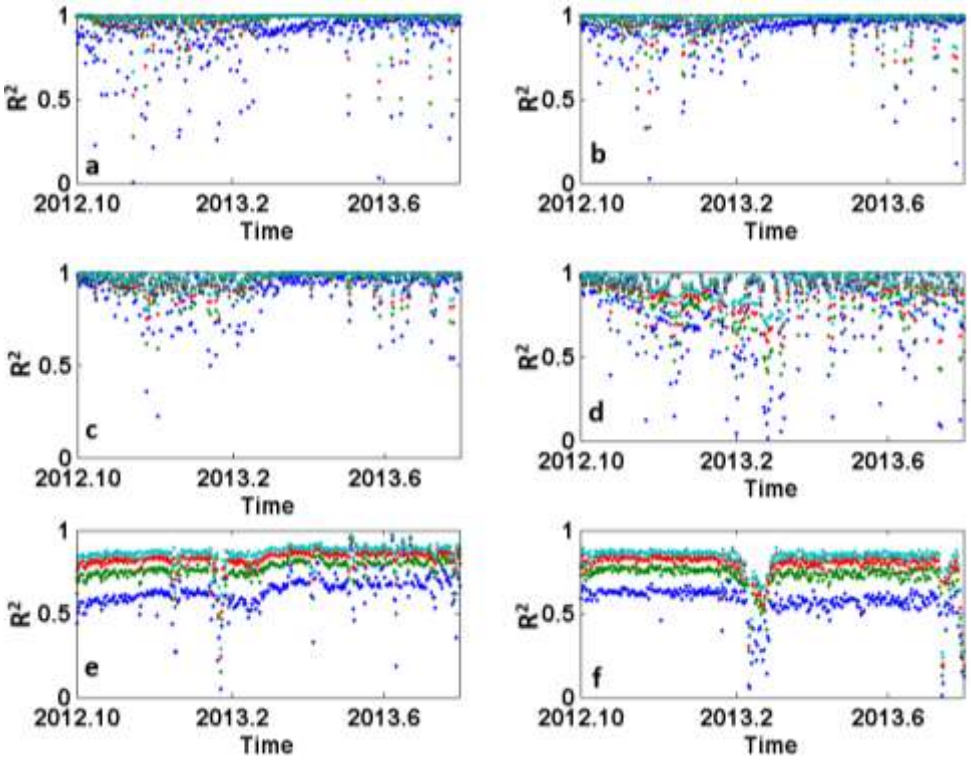

Fig. 9 Bias for soil temperature fitted by Fourier series. Results at **a**. 5 cm; **b**. 10 cm; **c**. 20 cm; **d**. 40 cm; **e**. 80 cm; and **f**. 180 cm. Dark blue for the 1st order, green for the 2nd order, red for the 3rd order, and light blue for the fourth order.

Fig. 10 Soil layer structure.

5 Conclusions

In this paper, the results of soil thermal diffusivities obtained from different boundary conditions under the thermal conduction equation are compared horizontally. A new model for solving the thermal diffusivity of the thermal conduction-convection equation under the Fourier boundary condition is proposed, and the results of soil temperature simulations with different order Fourier series are compared. The results show that (1) the amplitude method and phase method are based on a single temperature sine wave, which is used to describe the general soil; however, the accuracy is not high enough and the disadvantages are especially obvious when encountering multiple temperature extreme values. The logarithmic method and the arctangent method are performed four times a day, which can partially reflect the nonperiodic change of soil temperature; however, the data utilization rate is not high enough and the accuracy of the

obtained results is also low. The Laplace method does not have a clear soil temperature boundary function and thus can better address extreme weather effects or nonperiodic changes in soil temperature. (2) When solving the thermal conduction equation by a numerical method, format 2 (Crank-Nichalson-Sch format) is unconditionally stable and the data utilization rate is higher. The obtained soil thermal diffusivity is less discrete, and the result is more accurate. (3) When the thermal conduction-convection equation is used to solve the soil thermal diffusivity under the Fourier series boundary condition, the n-order soil thermal diffusivity k_n represents the influence of different fluctuations of soil temperature on the total soil thermal diffusivity and its contribution; when the soil temperature is simulated by the Fourier series, the result becomes more accurate as the order n becomes larger than the measured soil temperature. In addition, the Fourier series performs well in simulating and solving soil thermal properties. The model for solving the soil thermal diffusivity by the thermal conduction-convection equation under the Fourier boundary condition proposed in this paper has certain significance in solving the problem of thermal diffusivity calculation. However, it assumes that soil temperature changes have a certain periodicity, which may cause some problems when addressing nonperiodic changes in soil. According to the previous test, the Laplace method of the thermal conduction equation performs well in response to nonperiodic changes in soil temperature. However, the Laplace transform process is more difficult and the solution is more complicated. Therefore, this method should be applied to the thermal conduction-convection equation in a more convenient and feasible way, and it is expected to further contribute to the solution of soil thermal diffusivity.

Heat transport into active layer soils is important to understanding potential responses to changes in surface energy balance, particularly in the context of changing climate. Soil thermal properties are key parameters controlling the energy and water cycles. At the same time, with the global warming, near-surface air temperature acts as an external forcing of soil temperature, and its changes have a great impact on the thermal effects of soil fluctuations of different frequencies. Therefore, it is also necessary to analyze the thermal properties of soil fluctuations at different frequencies. This work starts with the improvement of soil thermal diffusivity, which is one of the thermal properties of soil. It helps to understand the changes in soil thermal properties and thermal movement, as well as the land-atmosphere interaction under the background of climate change.

Appendix

Derivation of $\boldsymbol{k_n}$ under Fourier series boundary condition (TCCMF)

According to the derivation of the conduction convection method by Gao (2005), we can derive the solution of the soil thermal diffusivity under Fourier series boundary conditions.

A_n^1, Φ_n^1 and A_n^2, Φ_n^2 under the Fourier series boundary condition can be expressed as follows:

$$A_n^1 = A_n \times z_1 e^{\left(-\frac{W}{2k}-\frac{\sqrt{2}}{4k}X_n\right)} \qquad (1'a)$$

$$\Phi_n^1 = \frac{\sqrt{2}\omega z_1}{nX_n} \qquad (1'b)$$

$$A_n^2 = A_n \times z_2 e^{\left(-\frac{W}{2k}-\frac{\sqrt{2}}{4k}X_n\right)} \qquad (1'c)$$

$$\Phi_n^2 = \frac{\sqrt{2}\omega z_2}{nX_n} \qquad (1'd)$$

where A_n^1, Φ_n^1 and A_n^2, Φ_n^2 are the amplitude and phase of the nth term of the Fourier series at depths z_1 and z_2, respectively; and $X_n = \sqrt{{W_n}^2 + \sqrt{{W_n}^4 + 16{k_n}^2\omega^2}}$.

Assuming that $z_1 > z_2$ (that is, $A_n^1 < A_n^2$, $\Phi_n^1 > \Phi_n^2$), the following is obtained:

$$\frac{\ln(A_n^1/A_n^2)}{z_1 - z_2} = \left(-\frac{W}{2k} - \frac{\sqrt{2}}{4k}X_n\right) \qquad (2')$$

From Eq. (1'b) and Eq. (1'd), the following can be concluded:

$$X_n = \frac{\sqrt{2}\omega(z_1 - z_2)}{n(\Phi_n^1 - \Phi_n^2)} \qquad (3')$$

Combining Eq. (2') with Eq.(3'), the following is obtained:

$$k_n^2 = \frac{(z_1 - z_2)^2 \cdot [W_n + \omega \cdot \frac{z_1 - z_2}{n(\Phi_n^1 - \Phi_n^2)}]^2}{4\ln^2(A_n^1/A_n^2)} = \frac{(z_1 - z_2)^2 \cdot [nW_n(\Phi_n^1 - \Phi_n^2) + \omega(z_1 - z_2)^2]}{4n^2(\Phi_n^1 - \Phi_n^2)^2\ln^2(A_n^1/A_n^2)} \qquad (4')$$

Eq. (4') can be rewritten as follows:

$$k_n^2 = \frac{(z_1 - z_2)^2}{4n^2(\Phi_n^1 - \Phi_n^2)^2}\left[\frac{\omega^2(z_1 - z_2)^2}{n^2(\Phi_n^1 - \Phi_n^2)^2} - W^2\right] \qquad (5')$$

Eq. (4') and Eq. (5') are combined to eliminate k_n and obtain an equation for W_n:

$$[nW_n(\Phi_n^1 - \Phi_n^2) + \omega(z_1 - z_2)]^2 = \ln^2\left(\frac{A_n^1}{A_n^2}\right)\left[\frac{\omega^2(z_1 - z_2)^2}{n^2(\Phi_n^1 - \Phi_n^2)^2} - W_n{}^2\right] \quad (6')$$

Eq. (6') can be rewritten as follows:

$$aW_n{}^2 + bW_n + c = 0 \quad (7')$$

where

$$\begin{cases} a = n^4(\Phi_n^1 - \Phi_n^2)^4 + n^2(\Phi_n^1 - \Phi_n^2)^2 \cdot \ln^2(A_n^1/A_n^2) \\ b = 2n^3\omega(\Phi_n^1 - \Phi_n^2)^3(z_1 - z_2) \\ c = \omega^2(z_1 - z_2)[n^2(\Phi_n^1 - \Phi_n^2)^2 - \ln^2(A_n^1/A_n^2)] \end{cases} \quad (8')$$

According to Eq. (7'), the value of W_n is not always negative:

$$W_n = \frac{\omega(z_1 - z_2)}{n(\Phi_n^1 - \Phi_n^2)}\left[\frac{2\ln^2\left(\frac{A_n^1}{A_n^2}\right)}{n^2(\Phi_n^1 - \Phi_n^2)^2 + \ln^2\left(\frac{A_n^1}{A_n^2}\right)} - 1\right] \quad (9')$$

$$k_n = -\frac{(z_1 - z_2)^2\omega\ln\left(\frac{A_n^1}{A_n^2}\right)}{n(\Phi_n^1 - \Phi_n^2)\left[n^2(\Phi_n^1 - \Phi_n^2)^2 + \ln^2\left(\frac{A_n^1}{A_n^2}\right)\right]} \quad (10')$$

Data availability statement

Datasets for this research are included in this paper (and its supplementary information files):

Yang, L., Gao, X., Lv, F., Hui, X., Ma, L., & Hou, X. (2017). Study on the local climatic effects of large photovoltaic solar farms in desert areas. Solar Energy, 144, 244–253. https://doi.org/10.1016/j.solener.2017.01.015

References

Ahmed N, Rao KR (1975) Orthogonal transforms for digital signal processing. Berlin, Heidelberg: Springer Science & Business Media

Bhumralkar CM (1975) Numerical experiments on the computation of ground surface temperature in an atmospheric general circulation model. J Appl Meteorol 14: 1246–1258. https://doi.org/10.1175/1520-0450(1975)014<1246:neotco>2.0.co;2

480 Carslaw HS, Jaeger JC (1959) Conduction heat in solids. Oxford, UK: Oxford Science
481 Publications.

482 de Silans AMBP, Monteny BA, Lhomme JP (1996) Apparent soil thermal diffusivity, a case
483 study: HAPEX-Sahel experiment. Agric For Meteorol 81: 201–216.
484 https://doi.org/10.1016/0168-1923(95)02323-2

485 Duan HD, Zhang XZ, Ma L, Li ZL, Zhang Z, Zhang ZG, Luo Y (2016) Fourier series sidereal
486 filtering in GPS dynamic deformation analysis. J Geod and Geodyn 36: 610–616

487 Fan XG, Tang MC (1994) A preliminary study on conductive and convection soil heat flux.
488 Plateau Meteorol 13: 14-19

489 Gao XQ, Yang LW, Lyu F, Ma LY, Li HL, Hui XY, Hou XH (2016) Observational study on the
490 impact of the large solar farm on air temperature and humidity in desert areas of Golmud.
491 Acta Energ Sol Sin 37: 2909–2915

492 Gao ZQ (2005) Determination of soil heat flux in a tibetan short-grass prairie. Bound Layer
493 Meteorol 114: 165–178. https://doi.org/10.1007/s10546-004-8661-5

494 Gao ZQ, Fan XG, Bian LG (2003) An analytical solution to one-dimensional thermal
495 conduction-convection in soil. Soil Sci, 168: 99–107. https://doi.org/10.1097/00010694-
496 200302000-00004

497 Goto S, Yamano M, Kinoshita M (2005) Thermal response of sediment with vertical fluid flow
498 to periodic temperature variation at the surface. J Geophys Res-Solid Earth 110: B01106.
499 https://doi.org/10.1029/2004jb003419

500 Halldin S, Gottschalk L, van de Griend AA, Gryning SE, Heikinheimo M, Hogstrom U, Jochum
501 A, Lundin LC (1998) NOPEX - a northern hemisphere climate processes land surface
502 experiment. J Hydrol 212: 172-187. https://doi.org/10.1016/S0022-1694(98)00208-X

503 Horton R, Wierenga PJ, Nielsen DR (1983) Evaluation of methods for determining the apparent
504 thermal diffusivity of soil near the surface. Soil Sci Soc Am J, 47: 25–32.
505 https://doi.org/10.2136/sssaj1983.03615995004700010005x

506 Hu GJ, Zhao L, Wu XD, Li R, Wu TH, Xie CW, Qiao YP, Shi JZ, Li WP, Cheng GD (2015)
507 New Fourier-series-based analytical solution to the conduction–convection equation to

calculate soil temperature, determine soil thermal properties, or estimate water flux. Int J Heat Mass Transf 95: 815–823. https://doi.org/10.1016/j.ijheatmasstransfer.2015.11.078

Hu YQ, Gao YX (1994). Some new understandings of processes at the land surface in arid area from the HEIFE. Acta Meteorol Sin 52: 286-296.

Hu YQ, Gao YX, Wang JM, Ji GL, Shen ZB, Cheng LS, Chen JY, Li SQ (1994) Some achievements in scientific research during HEIFE. Plateau Meteorol 13: 226-236

Kane DL, Hinkel KM, Goering DJ, Hinzman LD, Outcalt SI (2001) Non-conductive heat transfer associated with frozen soils. Glob Planet Change 29: 275–292. https://doi.org/10.1016/s0921-8181(01)00095-9

Lawford RG (1999) A midterm report on the GEWEX Continental-Scale International Project (GCIP). J Geophys Res-Atmos 104: 19279-19292. https://doi.org/10.1029/1999JD900266

Li NN, Jia L, Lu, J (2015) An improved algorithm to estimate the surface soil heat flux over a heterogeneous surface: A case study in the Heihe river basin. Sci Chin Earth Sci 58: 1169–1181. https://doi.org/10.1007/s11430-014-5041-y

Liang HQ (1982) Introducing into Fourier series a concept of coordinate set for analyzing signals in digital filters. Autom Electr Power Syst 3: 13–24

Liu QQ, Wei DP, Sun ZT, Han P (2014) Review of related researches on calculation of shallow ground heat transfer. Prog Geophys 29: 2510–2517

Liu SH, Cui Y, Liu HP (1991) Determination of thermal diffusivity of soil and its application. Quarterly J Appl Meteorol 2: 338–345

Seneviratne SI, Luthi D, Litschi M, Schar C (2006) Land-atmosphere coupling and climate change in Europe. Nature 443: 205-209. https://doi.org/ 10.1038/nature05095

Smith EA (1998) The first ISLSCP field experiment. J Atmos Sci 55: 1089-1090. https://doi.org/10.1175/1520-0469(1988)055<1089:TFIFE>2.0.CO;2

Van Wijk WR, de Vries DA (1963) Periodic temperature variations in a homogeneous soil. In: Van Wijk WR (ed) Physics of plant environment. Amsterdam: North-Holland Publishing Company, pp 103–143.

536 Wang LL, Gao ZQ, Horton R (2010) Comparison of six algorithms to determine the soil
537 apparent thermal diffusivity at a site in the Loess Plateau of China. Soil Sci 175: 51–60.
538 https://doi.org/10.1097/ss.0b013e3181cdda3f

539 Wang XP, Lin JX, Wu JW, Gao MJ (2019) Adaptive association rule mining algorithm based on
540 determination coefficient. CAAI Trans Intell Syst 15: 352-359.
541 https://doi.org/10.11992/tis.201809030

542 Williams KE, Harper AB, Huntingford C, Mercado LM, Mathison CT, Falloon PD, Cox PM,
543 Kim J (2019) How can the First ISLSCP Field Experiment contribute to present-day
544 efforts to evaluate water stress in JULESv5.0? Geosci Model Dev 12: 3207-3240.
545 https://doi.org/10.5194/gmd-12-3207-2019

546 Yang LW, Gao XQ, Lv F, Hui XY, Ma LY, Hou XH (2017) Study on the local climatic effects
547 of large photovoltaic solar farms in desert areas. Sol Energy 144: 244–253.
548 https://doi.org/10.1016/j.solener.2017.01.015

549 Zhang HH, Liu SH, Wei ZG, Lv SH, Hou XH, Wen J, Gao XQ (2011). Comparative study of
550 computing methods of soil temperature on different underlying surfaces. Acta Sci Nat
551 Univ Pekin 47: 1025–1033

552 Zheng H, Liu SH (2013) Land surface parameterization and modeling over desert. Chin J
553 Geophys 56: 2207–2217. https://doi.org/10.6038/cjg20130708

554